JOURNAL OF SOLID STATE CHEMISTRY 115, 435–440 (1995)

Magnetic Ordering in the Garnet $YCa_2SbFe_4O_{12}$

F. J. Berry,*,[1] J. Davalos,† C. Greaves,‡ J. F. Marco,† M. Slaski,§ P. R. Slater,‡ and M. Vithal*

*Department of Chemistry, The Open University, Milton Keynes MK7 6AA, United Kingdom; †Instituto de Quimica Fisica "Rocosolano," Consejo Superior de Investigaciones Cientificas, Serrano 119, 28006 Madrid, Spain; ‡School of Chemistry, University of Birmingham, Birmingham B15 2TT, United Kingdom; and §School of Physics, University of Birmingham, Birmingham B15 2TT, United Kingdom

Received April 18, 1994; in revised form July 15, 1994; accepted July 18, 1994

The magnetic order in $YCa_2[SbFe](Fe_3)O_{12}$ is very complex and field-dependent due to the substitution of diamagnetic Sb^{5+} ions on the octahedral sublattice. The magnetic behavior differs from that observed in $Y_2Ca[ZrFe](Fe_3)O_{12}$ presumably due to charge differences on the substituted cations. The main ferrimagnetic transition due to *a–d* coupling of the octahedral and tetrahedral sites is very broad and extends down to ca. 140 K. Below this temperature, the antiferromagnetic *d–d* exchange on the tetrahedral sites becomes significant and is thought to cause canting of the tetrahedral moments. At 10 K, the moments at both octahedral and tetrahedral sites determined by powder neutron diffraction—2.2(2) and 1.5(1) μ_B respectively—are very low and are consistent with significant canting on both cation sublattices. Mössbauer spectroscopy revealed five nonequivalent tetrahedral sites which relate to the occupation of nearest neighbor octahedral sites by a statistical distribution of Sb^{5+} and Fe^{3+} ions.

INTRODUCTION

Yttrium iron garnet, $Y_3[Fe_2](Fe_3)O_{12}$, has a ferrimagnetic framework structure of linked octahedra $[FeO_6]$ and tetrahedra (FeO_4) (1). The magnetic moments of the octahedral Fe^{3+} (two per formula unit in "*a*" sites of the structure) and tetrahedral Fe^{3+} (three per formula unit, "*d*" sites) are antiferromagnetically coupled to provide a spontaneous moment of around 5.0 μ_B per mole (see, for example (2)). Since the order of antiferromagnetic exchange interactions is *a–d* > *d–d* > *a–a* (see, for example (3, 4)), the substitution of diamagnetic ions on either of the Fe sublattices can weaken the *a–d* interactions and provide quite complex magnetic structures. A magnetic model (3) has been shown to provide a satisfactory explanation of the magnetic properties of substituted garnets such as $Y_{3-x}Ca_x[Fe_2](Fe_{3-x}Si_x)O_{12}$ and $Y_{3-x}Ca_x[Zr_xFe_{2-x}](Fe_3)O_{12}$. In this model, gradual transformations from the *a–d* ferrimagnetic $Y_3Fe_5O_{12}$ to the *a–a* and *d–d* antiferromagnets $Ca_3[Fe_2](Si_3)O_{12}$ and $YCa_2[Zr_2](FeO_3)O_{12}$ occur via the canting of magnetic moments on the unsubstituted sublattice at intermediate compositions, as shown schematically in Fig. 1. In accordance with this model, which was further developed by Rosencwaig (5, 6), the observed spontaneous moments for $Y_2Ca[ZrFe](Fe_3)O_{12}$ (5.2 μ_B) and $Y_3[ScFe](Fe_3)O_{12}$ (5.7 μ_B) are indicative of significant reductions in the tetrahedral Fe^{3+} moments (to 3.4 and 3.6 μ_B respectively) due to canting of the moments by an average of ca. 45° from the direction antiparallel to the octahedral Fe^{3+} moments. The model has proved valuable for explaining the magnetic properties of several substituted garnets (3), and we have examined its applicability to a new garnet containing the partial substitution of Sb^{5+} ions on the octahedral Fe^{3+} sublattice. In this paper we report the synthesis of $YCa_2[SbFe](Fe_3)O_{12}$ and its structural and magnetic characteristics determined using magnetization measurements, Mössbauer spectroscopy, and powder neutron diffraction (PND).

EXPERIMENTAL

The compound $YCa_2[SbFe](Fe_3)O_{12}$ was made by sequential heating of a thoroughly ground stoichiometric mixture of high purity $CaCO_3$, Y_2O_3, Sb_2O_3, and Fe_2O_3 at 500°C (4 hr), 900°C (2 hr), and finally at 1210°C (24 hr) in air. Repeated heating at 1210°C gave a garnet-related product which was shown to be single phase by a full Rietveld structure refinement based on powder X-ray diffraction data. Allowing the cation site occupancies to vary confirmed that the composition corresponded to that expected for the initial mixture of reactants.

Iron-57 Mössbauer spectra were recorded at temperatures between 18 and 298 K using a constant acceleration Mössbauer spectrometer with a $^{57}Co/Rh$ source and a helium closed-cycle cryogenerator. The powdered sample was sandwiched between two aluminum foils to ensure good thermal conductivity between the sample and sample holder. Temperature control was achieved within ±1.5 K. The spectra recorded at 298 and 18 K were computer fitted to Lorentzian lines using the usual constraints of equal area and width for the two lines of doublets, and

[1] To whom correspondence should be addressed.

0022-4596/95 $6.00

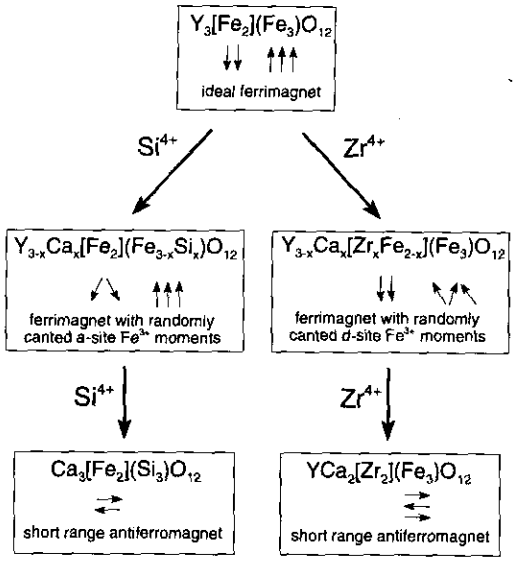

FIG. 1. Schematic representation of magnetic order in substituted garnets (after Geller (3)).

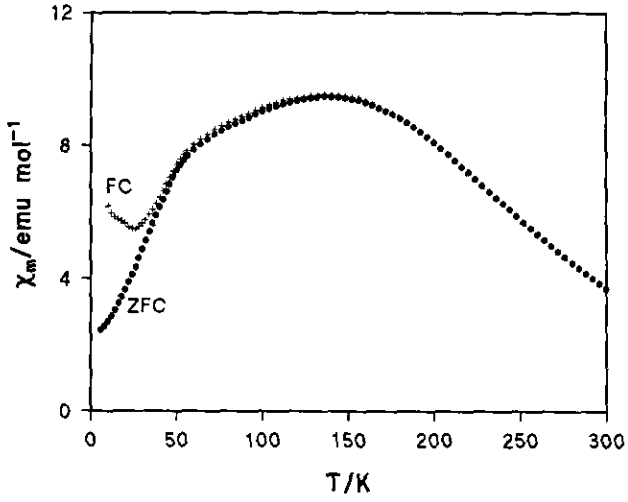

FIG. 2. Field-cooled (FC) and zero-field-cooled (ZFC) magnetic susceptibilities per mole Fe^{3+} measured at 5×10^{-4} T.

of equal width and areas in the ratio 3:2:1:1:2:3 for the six lines of sextets. The chemical isomer shift data are referred to α-iron. The magnetic ordering temperature was determined by thermoscanning experiments in which the transmission of the 14.4 keV gamma rays were measured at different temperatures with a stationary source (7).

Magnetic susceptibility measurements were made using a Cryogenics S100 SQUID susceptometer and an Oxford Instruments VSM. PND data were collected (24 hr at temperatures of 295, 50, and 10 K) from a 10-g sample contained in a cylindrical vanadium can using neutrons of wavelength 2.3737 Å on the TAS3 diffractometer at Risø, Denmark. Nuclear and magnetic contributions to the scattering were analyzed simultaneously using the Rietveld method after manual subtraction of the background. The free ion form factor for magnetic scattering from Fe^{3+} was assumed (8).

RESULTS AND DISCUSSION

The variation of magnetic susceptibility of $YCa_2[SbFe](Fe_3)O_{12}$ with temperature, determined from SQUID measurements, is shown in Fig. 2. On cooling, a very broad ferrimagnetic transition is observed which begins above 300 K and the susceptibility peaks at ca. 140 K before decreasing at lower temperatures. Although at low applied fields (e.g., 5 G {5×10^{-4} T}, Fig. 2), the field-cooled (FC) and zero-field-cooled (ZFC) susceptibilities deviated at temperatures below ca. 40 K due to irreversibility effects, VSM measurements demonstrated that at higher applied fields (>10^4 G {1 T}), the FC and ZFC susceptibilities were coincident, and no decrease in susceptibility occurred below the peak at 140 K. Field sweeps up to 1 T at 6 and 150 K produced very similar results and showed a high degree of reversibility and a small coercive force, as seen in Fig. 3. Extrapolation of the high field magnetic moment to zero field yielded a saturation moment of 3.0(1) μ_B, which is significantly lower than the value of 5.2 μ_B reported for the related $Y_2Ca[ZrFe](Fe_3)O_{12}$ (3). Given these interesting magnetic phenomena, the magnetic properties of this phase were examined further using PND and Mössbauer spectroscopy.

Structure refinement based on the ambient temperature PND data supported X-ray diffraction results and con-

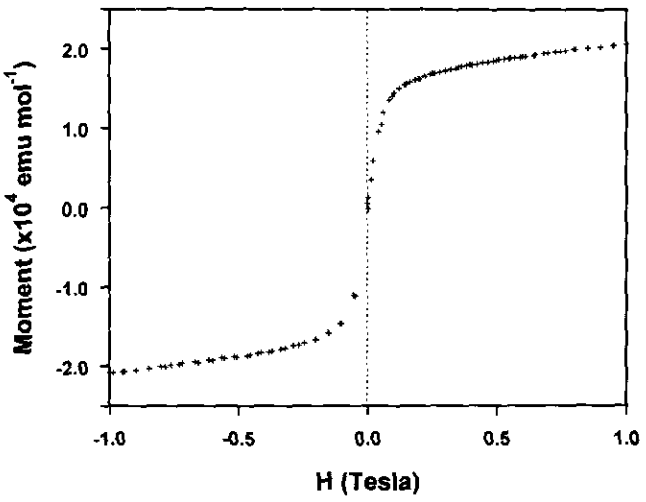

FIG. 3. Magnetization of $YCa_2[SbFe](Fe_3)O_{12}$ in fields swept from −1 to 1 T at 150 K.

TABLE 1
Refined Structural and Magnetic Parameters for $YCa_2[SbFe](Fe_3)O_{12}$ Obtained from Neutron Diffraction at 10 K

Atom	Position	x	y	z	B (Å^2)	Cell occupancy
Y/Ca	24*c*	$\frac{1}{8}$	0	$\frac{1}{4}$	0.8(2)	24
Sb/Fe(1)	16*a*	0	0	0	0.5(1)	16
Fe(2)	24*d*	$\frac{3}{8}$	0	$\frac{1}{4}$	0.1(1)	24
O(1)	96*h*	0.9711(2)	0.0535(2)	0.1486(2)	0.3(1)	96
O(2)	96*h*	0.0289(2)	0.9465(2)	0.8514(2)	0.3(1)	96

Magnetic moments:
Fe(1) $-2.2\ \mu_B$; Fe(2) $1.5(1)\ \mu_B$
Overall moment $2.3(4)\ \mu_B$ per mole.

Space group $Ia3d$, $a = 12.521(1)$ Å.
$R_{wp} = 12.6\%$, $R_p = 12.4\%$, $R_E = 7.4\%$, $R_I{}^a = 2.9\%$, $R_M{}^a = 6.2\%$

[a] R_I and R_M are conventional integrated intensity R factor estimates for nuclear and magnetic contributions to the profile, respectively.

firmed the presence of Sb at only the octahedral *a* sites of the garnet structure. However no magnetic component to the neutron scattering was detectable, and the weak magnetic order at this temperature was therefore assumed to extend over only short distances. The data sets collected at 10 K and 50 K appeared identical with some low-angle reflections being slightly more intense than in the 295 K data set, and this was attributed to magnetic scattering. To simplify the refinement, a common isotropic temperature factor was assigned to both oxygen sites, and the full results of the nuclear and magnetic refinements derived from the 10 K data are given in Table 1, with the fitted profiles shown in Fig. 4. The most significant feature of the refinement is the very low moments for both the octahedral (Fe(1), $2.2(2)\ \mu_B$) and tetrahedral (Fe(2), $1.5(1)\ \mu_B$)) ions, compared with the expected free ion value of $5.0\ \mu_B$. Although the small moments provide an imprecise estimate of the resultant magnetic moment

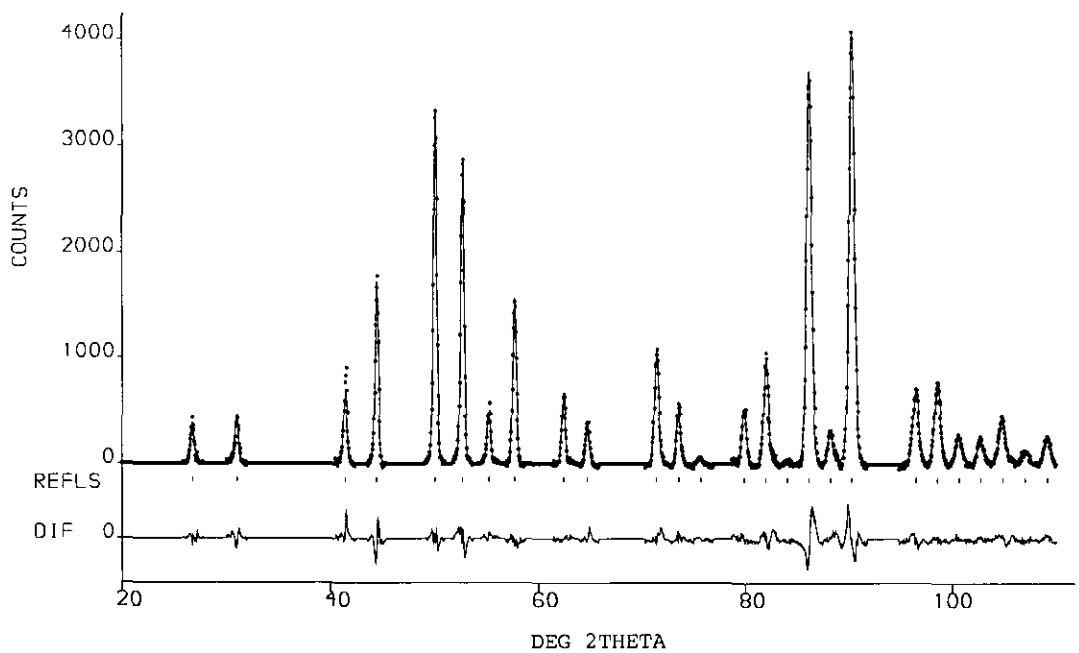

FIG. 4. Observed, calculated, and difference neutron diffraction profiles for $YCa_2[SbFe](Fe_3)O_{12}$ at 10 K.

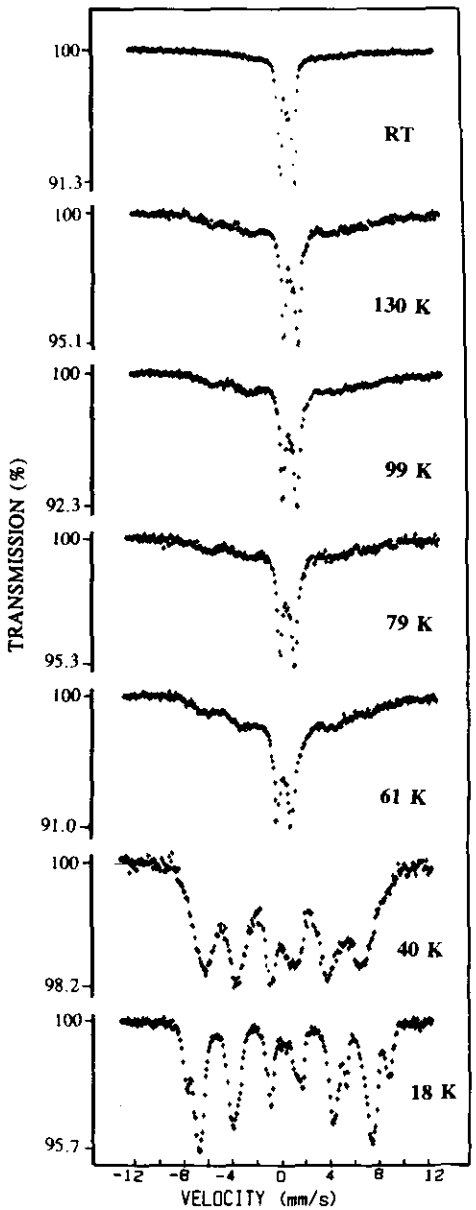

FIG. 5. Mössbauer spectra of $YCa_2[SbFe](Fe_3)O_{12}$ between 298 and 18 K.

at 2.3(4) μ_B, this is in reasonable agreement with the SQUID measurements. A reduction in the tetrahedral moment is in accordance with canting of these moments resulting from the effects of *d–d* antiferromagnetic exchange as previously suggested and as represented schematically in Fig. 1. However, the moment is very low and corresponds to a canting angle of 73° from the direction of the overall magnetic polarization vector. It is more difficult to understand the substantial reduction in moment at the octahedral Fe(1) positions indicated by the neutron diffraction data. Canting could be responsible, but such an effect has not previously been observed and no clear mechanism is apparent. Alternatively, the reduction could be associated with incomplete magnetic order, which may be attributed to inhomogeneities in the distribution of Fe^{3+} and Sb^{5+} ions on these sites. In this way, islands of magnetic order formed within a disordered sea would result in a reduction in the experimental moments at both the octahedral and the tetrahedral sites.

At 298 K, the ^{57}Fe Mössbauer spectra showed the presence of Fe^{3+} in both octahedral and tetrahedral sites (Figs. 5 and 6). The spectra recorded at 130, 99, and 79 K (Fig. 5) were very similar and showed the presence of a weak magnetic component, which gradually increased in intensity at the expense of the paramagnetic species. This observation is consistent with the SQUID measurements and suggests a very gradual ordering process. This coexistence of a doublet and a magnetic component over a broad temperature range has been observed in other diamagnetically substituted iron-containing garnets (4, 9, 10) and explained in terms of critical superparamagnetism (4, 9–11). According to this model, in the low temperature region where the doublet and magnetic spectral components coexist, the crystal is composed of magnetically independent areas; the stable larger regions are magnetically fully ordered and give the sextet pattern, while the smaller regions originate from iron in short-range ordered clusters and give the central doublet (9). The intensity of the magnetic component increased rapidly below 79 K and no paramagnetic ions were apparent at 18 K. The weak absorption at 0 mm s^{-1} results from an impurity in the aluminum foil sample holder. The absence of a paramagnetic component at this temperature is indicative

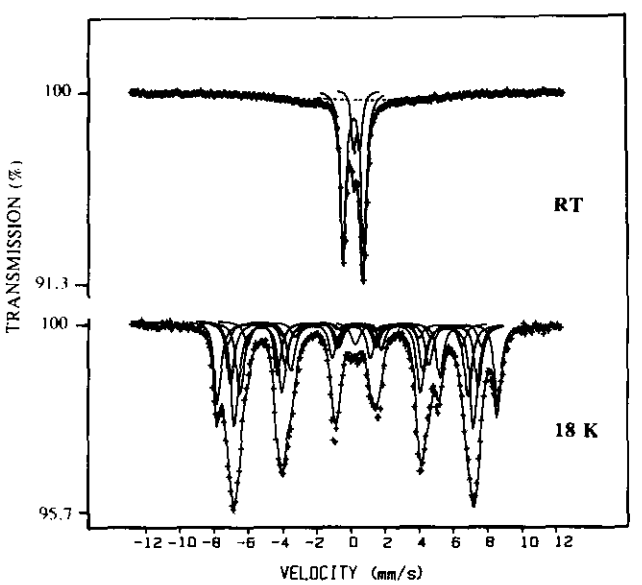

FIG. 6. Unconstrained fits to the Mössbauer spectra of $YCa_2[SbFe](Fe_3)O_{12}$ at 298 and 18 K.

TABLE 2
^{57}Fe Mössbauer Parameters for $YCa_2[SbFe](Fe_3)O_{12}$ at 18 K Using Unconstrained Fitting Procedures

	Species	$\delta \pm 0.01$ (mm/sec)	$\Delta \pm 0.02$ (mm/sec)	$\Gamma \pm 0.02$ (mm/sec)	$H \pm 5$ (kG)	I_{obs} (%)	I_{calc} (%)[b]
298 K	Fe_{tet}	0.17	1.21	0.37	—	78	75
	Fe_{oct}	0.37	0.37	0.29	—	22	25
18 K	$Fe_{tet}(0)$[a]	0.37	−0.11	0.55	392	6	4.5
	$Fe_{tet}(1)$[a]	0.38	−0.16	0.57	419	23	19
	$Fe_{tet}(2)$[a]	0.22	0.21	0.51	439	25	28
	$Fe_{tet}(3)$[a]	0.38	−0.15	0.57	456	20	19
	$Fe_{tet}(4)$[a]	0.37	−0.15	0.55	465	6	4.5
	Fe_{oct}	0.53	−0.05	0.48	514	20	25

[a] The number in parentheses indicates the number of neighboring octahedral sites occupied by Fe.
[b] Estimated assuming a random distribution of octahedral Fe and Sb ions.

of a uniform magnetic structure extending throughout the solid, and suggests that the low octahedral moment deduced from neutron scattering most probably reflects a genuine canting of the moments due to magnetic frustration. The spectrum at 40 K showed magnetic order over both the tetrahedral and octahedral sites, but significant relaxation is indicative of incomplete magnetic order.

The data recorded at 18 K were fitted to one sextet corresponding to Fe^{3+} in octahedral sites and five sextets corresponding to Fe^{3+} in tetrahedral sites. In this compound, all the tetrahedral sites are occupied by Fe^{3+} but half the octahedral sites are occupied by Fe^{3+} and half by Sb^{5+}. Each octahedral Fe^{3+} is linked through oxygen to six tetrahedrally coordinated Fe^{3+} such that all the octahedral sites are expected to have identical environments. However, this is not the case for the tetrahedrally coordinated Fe^{3+} ions which are linked to four octahedral sites containing a statistical distribution of Fe^{3+} and Sb^{5+} ions. In this way, five nonequivalent tetrahedral sites are expected, corresponding to the following configurations of neighboring octahedra:

$$4Fe^{3+};\ 3Fe^{3+} + 1Sb^{5+};\ 2Fe^{3+} + 2Sb^{5+};$$
$$1Fe^{3+} + 3Sb^{5+};\ 4Sb^{5+}.$$

Hence the data were fitted to this model (12, 13) and the results are shown in Fig. 6 and Table 2. The intensities are in satisfactory agreement with those expected for a random distribution of Fe^{3+} and Sb^{5+} over the octahedral sites, as shown in Table 2. Finally, a plot of γ-ray transmission at zero velocity against temperature (Fig. 7) indicated the principal magnetic ordering to occur at ca. 75 K, which appears to correspond primarily to the onset of the *d–d* antiferromagnetic interactions on the tetrahedral sublattice which cause canting of the tetrahedral moments.

The combination of PND, magnetic susceptibility measurements, and Mössbauer spectroscopy has confirmed $YCa_2[SbFe](Fe_3)O_{12}$ to have a random distribution to Sb and Fe ions on the octahedral sites of the garnet structure. Magnetic ordering is frustrated by the diamagnetic Sb ions, and the ferrimagnetic ordering between octahedral and tetrahedral Fe^{3+} ions therefore extends over a wide temperature range. At temperatures below 140 K, Mössbauer spectra were indicative of the coexistence of two magnetically independent regions in the crystals. In this temperature range, antiferromagnetic exchange between the tetrahedral Fe^{3+} cations becomes significant and causes canting of the moments, and PND data recorded at 10 K suggest substantial reductions in the magnetic moment for both octahedral and tetrahedral Fe^{3+} species.

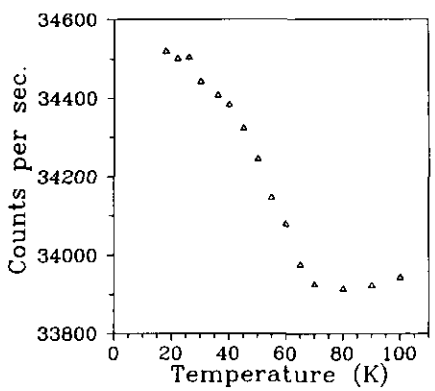

FIG. 7. Variation of γ-ray transmission at zero velocity with temperature.

ACKNOWLEDGMENTS

We thank SERC for financial support and B. Lebech for experimental assistance with collecting the neutron diffraction data.

REFERENCES

1. S. Geller, *Z. Kristallogr.* **125,** 1 (1967).
2. M. Bonnet, A. Delapalme, P. Becker, and H. Fuess, *J. Magn. Magn. Mater.* **7,** 23 (1978).
3. S. Geller, *J. Appl. Phys.* **37,** 1408 (1966).
4. A. P. Dodokin, I. S. Lyubutin, B. V. Mill, and V. P. Peshkov, *Sov. Phys. JETP* **36,** 526 (1973).
5. A. Rosencwaig, *Can. J. Phys.* **48,** 2857 (1970).
6. A. Rosencwaig, *Can. J. Phys.* **48,** 2868 (1970).
7. R. S. Preston, S. S. Hanna, and J. Herberle, *Phys. Rev.* **128,** 542 (1962).
8. R. E. Watson and A. J. Freeman, *Acta Crystallogr.* **14,** 27 (1961).
9. J. Piekowszewski and J. Suwalski, *in* "Proceedings, Conference on Applications of The Mössbauer Effect," Tihany, Hungary, 1969, (I. Dezsi, Ed.), p. 499. Academiai Kiado, Budapest, 1971.
10. J. M. D. Coey, *Phys. Rev. B* **6,** 3340 (1972).
11. Y. Ishikawa, *J. Appl Phys* **35,** 1054 (1964).
12. V. A. Bokov, S. I. Jushchuk, and G. V. Popov, *Solid State Commun.* **7,** 373 (1969).
13. V. A. Bokov, G. V. Popov, and S. I. Jushchuk, *Sov. Phys. Sol. State* **11,** 479 (1969).